JOURNAL OF GEOPHYSICAL RESEARCH, VOL. 99, NO. B9, PAGES 18,109–18,116, SEPTEMBER 10, 1994

Strain accumulation along the Laguna Salada fault, Baja California, Mexico

J. C. Savage, M. Lisowski, N. E. King, and W. K. Gross

U.S. Geological Survey, Menlo Park, California

Abstract. Strain accumulation observed over the 1978–1991 interval in a 30 × 100 km aperture trilateration network spanning the Laguna Salada fault is described by the principal strain rates 0.101 ± 0.012 μstrain/yr N80°E±2° and −0.021 ± 0.012 μstrain/yr N10°W±2°, extension reckoned positive. These strain accumulation rates have been corrected to remove coseismic effects of the nearby 1979 Imperial Valley (M = 6.5), 1980 Victoria (Baja California) (M = 6.4), 1987 Superstition Hills (M = 6.5), and 1987 Elmore Ranch (M = 5.9) earthquakes. The observed strain rates indicate extension at a rate of about 0.08 μstrain/yr perpendicular to the trend (N35°W) of the Salton trough as well as a right-lateral tensor shear strain rate 0.05 μstrain/yr across it. The extension perpendicular to the trough is observed neither farther north near the Salton Sea nor farther south across the Gulf of California. However, Holocene slip on the Laguna Salada fault, about equal parts right-lateral and normal slip, is consistent with the observed strain accumulation. A simple dislocation model intended to explain the observed strain accumulation as a product of slip at depth on the Laguna Salada fault would require that the fault be listric.

Introduction

In 1978 the U.S. Geological Survey established a geodetic network just south of the U.S.-Mexico border to measure strain accumulation along the Laguna Salada fault (Figure 1). The Laguna Salada fault is the southward continuation into Mexico of the Elsinore fault in United States. The Elsinore-Laguna Salada fault system is thought to carry about 5 mm/yr of relative plate motion from near the north end of the Gulf of California into the Los Angeles basin, bypassing the San Andreas fault system in southern California [*Humphreys and Weldon*, 1991]. The Laguna Salada fault itself exhibits clear evidence of oblique slip, with roughly equal components of normal and right-lateral slip during the Holocene [*Mueller and Rockwell*, 1991]. A recently formed, 25-km-long scarp along the fault trace (Figure 1) was apparently the product of the February 23, 1892, M = 7 earthquake known to have occurred in that vicinity [*Mueller and Rockwell*, 1991]. A M = 6.5 earthquake occurred on December 30, 1934, somewhat farther south along the Chupamiertos segment of the Laguna Salada fault system (Figure 1).

Line Length Measurements

The Laguna Salada network (Figure 1) was surveyed twice in 1978, twice in 1979, once in 1981, and once in 1991. In each survey a Geodolite, a precise electro-optical distance measuring instrument, was used to determine the distance from one geodetic station to another. The distances measured are indicated by lines in Figure 1. A refractivity correction is required for each measurement to adjust for the actual velocity of light along the observed line. The refractivity correction is determined from end-point pressure measurements and humidity and temperature profiles measured along the line of sight from a small airplane at the time of ranging. *Savage and Prescott* [1973] have discussed the procedures used and the accuracy obtained in such surveys. The standard deviation of a measured length L is

$$\sigma = (a^2 + b^2 L^2)^{1/2} \quad (1)$$

where a = 3 mm and $b = 0.2 \times 10^{-6}$ (dimensionless). This estimate of error may be further resolved into random and systematic components. Both of these components are described by standard deviations of the form (1) with a = 3 mm and $b = 0.14 \times 10^{-6}$ (dimensionless) for the random component and a = 0.5 mm and $b = 0.14 \times 10^{-6}$ (dimensionless) for the systematic component [*Savage et al.*, 1986, pp. 7459–7460]. The systematic error is principally due to imperfect calibration of the meteorological probes used to measure pressure, temperature, and humidity needed for the refractivity correction. Because these probes are replaced or recalibrated between surveys, the associated error is systematic in any one survey but only randomly related to the systematic error in a subsequent survey.

Paper number 94JB01471.

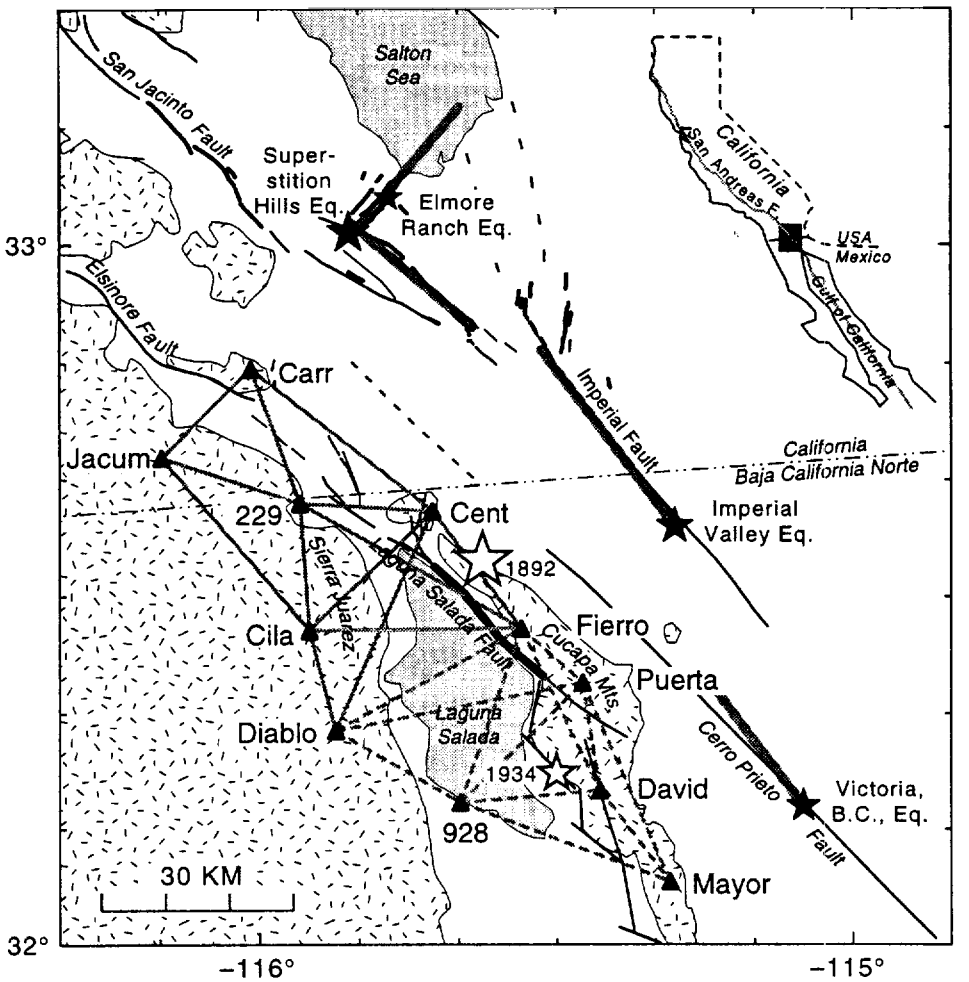

Figure 1. Map showing Laguna Salada trilateration network (lines connecting triangles), principal faults (sinuous lines), and earthquake epicenters (stars). Shaded bars show the extent of rupture associated with five of the earthquakes. The patterned areas correspond to mountain ranges. Epicenter locations from *Ellsworth* [1990] and map base from *Mueller and Rockwell* [1991, Figure 1].

Measurements

In the 1978–1991 interval, over which deformation of the Laguna Salada network was measured, four moderate earthquakes (Imperial Valley: October 15, 1979, $M = 6.5$; Victoria, Baja California: June 9, 1980, $M = 6.4$; Superstition Hills: November 24, 1987, $M = 6.5$; and Elmore Ranch: November 24, 1987, $M = 5.9$) occurred along a northwestward trend paralleling the network (Figure 1). Those earthquakes occurred sufficiently close to the Laguna Salada network to cause coseismic changes in the network. We have constructed dislocation models for those earthquakes (Table 1) and calculated the coseismic changes in length of each of the 25 lines in the Laguna Salada network due to the two pairs of earthquakes, the Imperial Valley-Victoria pair and Superstition Hills-Elmore Ranch pair (Table 2). Those coseismic changes were then removed from all line lengths measured after the respective earthquake pairs. Thus, the line-length data discussed here should reflect only the effects of interseismic strain accumulation.

The corrected line-length data are plotted in Figure 2 as a function of time. The three lines (Carr to Jacum and 229 and Jacum to 229) wholly within the United States were more accessible to the U.S. Geological Survey crews and therefore surveyed more frequently than the other lines. A linear fit to the data for each line is shown in the figure. The slopes of those lines obviously depend heavily upon the 1991 observation. However, the more complete data sets for the three lines wholly within the United States indicate no particular problem with the 1991 survey. Notice that seven measurements (circled in Figure 2) out of station 928 lie more than two standard errors from the linear fit. However, six of those measurements are accompanied by another measurement in the same year that lies within two standard errors of the linear fit. Thus, we conclude that the corrected line-length measurements are consistent with deformation that is uniform in time. Moreover, though it is not shown in the figure, the coseismic corrections, some as large as 30 mm, do reduce the scatter in the data about a linear trend.

The average rates of change of line length (slopes of

Table 1. Rupture Parameters Used in Modeling the Effects of Four Nearby Earthquakes

Parameter	Earthquake			
	Imperial*	Victoria†	Superstition Hills‡	Elmore Ranch‡
Strike	N37°W	N37°W	N50°W	N40°E
Dip, deg	80°NE	90	90	90
Length, km	35	23	25	25
Depth to top, km	5	5	0	0
Downdip width, km	8	8	10	10
Trace midpoint				
Latitude, °N	32.71	32.28	32.96	33.11
Longitude, °W	115.40	115.19	115.74	115.75
Right-lateral slip, m	0.8	0.9	1.3	−0.3
Moment, 10^{17}Nm	67.2	49.7	97.5	22.5
Equiv. Magnitude	6.5	6.4	6.6	6.2

*Archuleta [1984].
†*Lisowski and Prescott* [1984] and *Silver and Masuda* [1985].
‡*Larsen et al.* [1992].

the linear fits to the line-length data in Figure 2) are shown in Table 2. Only nine of the 25 rates are significantly (two standard deviations) different from zero. Nevertheless, we will show in the next section that the rates exhibit a systematic pattern when divided by line length and plotted as a function of azimuth (Figure 3).

Strain Accumulation

The overall deformation of the Laguna Salada network is adequately described by the uniform strain rate field that best approximates the observed line-length changes. That is, we assume that the line-length changes occur linearly with time (Figure 2) and find the uniform-in-space strain rate that best approximates the observed line-length changes. That strain rate is shown in Table 3. The strain rate components $\dot{\epsilon}_{ij}$ are the tensor components referred to a geographic coordinate system (i.e., the 1 axis directed east and the 2 axis north), whereas the components $\dot{\epsilon}'_{ij}$ are referred to a coordinate system rotated 40° counterclockwise from the geographic system so that the 1′ axis is normal to the trend of the Laguna Salada fault and the 2′ axis is

Table 2. Coseismic Corrections to Line Length and Average Rate of Change of Corrected Line Length (dL/dt)

From	To	Length, km	Aximuth, deg	Imperial, Victoria, mm	Sup. Hills-Elmore, mm	dL/dt, mm/yr
928	David	22.4	84.9	−13.1	−0.6	1.6±1.4
	Diablo	22.9	120.5	−3.4	0.3	1.6±0.7
	Fierro	29.3	19.4	14.4	8.9	−0.1±0.9
	Mayor	35.7	110.6	4.9	1.7	2.8±0.7
	Puerta	27.4	45.5	2.1	1.0	1.8±1.1
Carrizo	Cent	36.4	128.2	−7.8	−0.1	0.7±0.9
	Jacum	19.9	44.7	−2.4	−21.2	1.3±0.4
	229	22.7	160.1	0.0	−9.1	−1.1±0.4
Cent	Cila	27.1	45.8	−5.7	22.0	1.8±0.5
	Diablo	37.9	23.9	−3.8	34.3	1.1±0.7
	Fierro	23.3	142.8	−9.4	24.7	0.4±0.5
	229	20.9	93.3	−5.8	−1.5	3.2±0.5
Cila	Diablo	16.3	165.3	−0.8	4.0	−0.1±0.4
	Fierro	33.5	89.5	−1.9	−2.5	4.0±0.7
	Jacum	35.9	139.6	−1.6	10.2	0.9±0.7
	229	20.2	175.8	−1.4	7.3	0.5±0.4
David	Fierro	28.6	154.0	4.2	11.4	−0.6±0.6
	Mayor	18.3	142.7	4.4	2.8	0.9±0.5
	Puerta	17.4	171.0	16.3	4.5	−0.5±0.4
Diablo	Fierro	33.6	61.4	5.8	1.7	3.2±0.8
	Puerta	40.0	79.1	−15.0	−1.6	4.4±0.9
Fierro	229	40.2	119.4	−8.6	1.8	3.3±1.1
	Puerta	12.9	130.9	−15.6	5.5	0.3±0.4
Mayor	Puerta	34.7	156.5	13.4	7.5	0.4±0.7
Jacum	229	22.9	108.4	−4.9	3.8	0.8±0.4

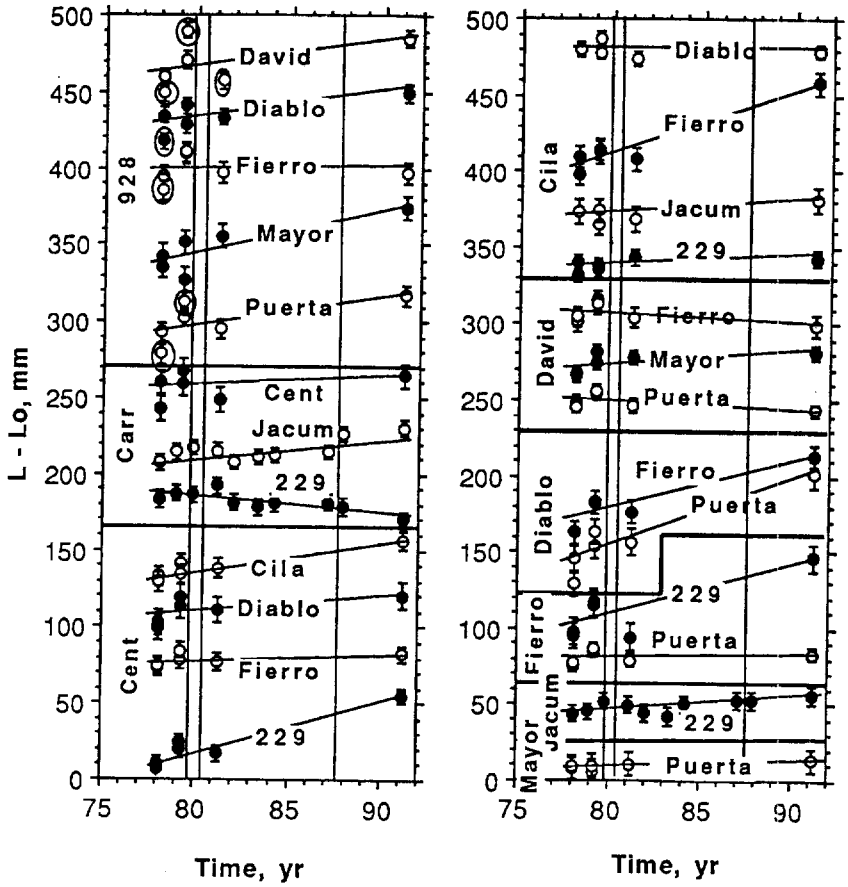

Figure 2. The corrected line length L less a constant nominal length plotted as a function of time. The error bars represent one standard deviation on either side of the plotted points. A linear fit to the data for each line is shown. Data points more than two standard deviations from the linear fit are circled. Vertical lines identify times of the Imperial Valley, Victoria, and Superstition Hills-Elmore Ranch earthquakes.

parallel to it. The $\dot{\varepsilon}_1$ and $\dot{\varepsilon}_2$ strain rates are the principal strain rates; the azimuth of the principal extension rate is given in the last row of the table. Extension is reckoned positive for all strain rates. The observed strain rate is approximately described as a N80°E uniaxial 0.10 ± 0.01 μstrain/yr extension.

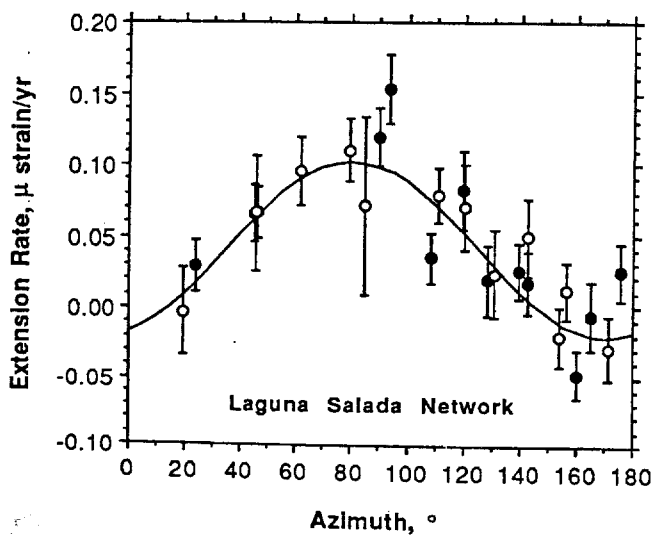

The spatial uniformity of the strain rate can be tested by comparing the strain rates determined for the north half and south half of the network separately. The network has been divided into a north half (solid lines) and south half (dashed lines) in Figure 1. Notice that no line is common to both halves. The strain rates determined for the two halves are shown in Table 3; they do not differ significantly.

The uniformity of the deformation of the network can be demonstrated in another way. The extension rates ($L^{-1}dL/dt$ from Table 2) for the individual lines are plotted as a function of the azimuth in Figure 3. The extension rate at each azimuth predicted by the uniform strain rate fit in Table 3 is shown as a sinusoid in

Figure 3. Corrected extension rates ($L^{-1}dL/dt$) for the individual lines plotted as a function of azimuth. The sinusoid represents the extension rate predicted by the best fitting uniform strain rate (Table 3). The error bars represent one standard deviation on either side of the plotted point. Rates for lines in the south half of the network (dashed lines in Figure 1) are represented by open circles whereas rates for lines in the north half are shown by solid circles.

Table 3. Corrected Strain Rates With Standard Deviation

Strain Rate, μstrain/yr	Whole Network	North Half	South Half
$\dot{\varepsilon}_{11}$	0.098±0.012	0.104±0.013	0.107±0.015
$\dot{\varepsilon}_{12}$	0.020±0.004	0.027±0.006	0.013±0.007
$\dot{\varepsilon}_{22}$	−0.018±0.012	−0.018±0.013	−0.009±0.016
$\dot{\varepsilon}'_{11}$	0.070±0.012	0.080±0.014	0.072±0.015
$\dot{\varepsilon}'_{12}$	−0.053±0.005	−0.055±0.007	−0.055±0.008
$\dot{\varepsilon}'_{22}$	0.010±0.011	0.006±0.012	0.026±0.015
$\dot{\varepsilon}_1$	0.101±0.012	0.110±0.014	0.108±0.015
$\dot{\varepsilon}_2$	−0.021±0.012	−0.023±0.013	−0.010±0.016
Azimuth Principal Extension	N80.3°E±2.1°	N78.1°E±2.6°	N83.6°E±3.4°

Here, $\dot{\varepsilon}_{ij}$ are referred to a geographic coordinate system (1 axis directed east and 2 axis north); $\dot{\varepsilon}'_{ij}$ are referred to a coordinate system rotated 40° counterclockwise from the geographic; $\dot{\varepsilon}_1$ and $\dot{\varepsilon}_2$ are the principal strain rates.

that figure. The extension rates predicted by the uniform strain rate approximation furnish a good fit to the observed extension rates.

Dislocation Modeling

Strain accumulation along a fault is generally attributed to aseismic slip at depth on that fault [*Savage*, 1983], a process readily modeled by dislocations in an elastic half-space. Here we attempt to construct such a model using a planar fault to account for the deformation observed along the Laguna Salada fault. We have only limited success in fitting the data using a conventional planar fault model. *Savage et al.* [1992] encountered a similar difficulty in modeling strain accumulation across the Wasatch fault, a normal fault in Utah. In both cases an acceptable fit could be obtained using a listric fault model. However, the data are not adequate to demonstrate that slip at depth on the Laguna Salada fault is in fact the source of the observed strain accumulation.

In the dislocation model the Laguna Salada fault is represented by a throughgoing cut in the elastic half-space dipping 60° S50°W from the trace of the actual fault as mapped on the half-space surface. The nearby plate-boundary fault system (San Andreas, San Jacinto, Imperial, and Cerro Prieta faults) is represented by a single, throughgoing vertical cut striking N37°W through the epicenter of the Imperial Valley earthquake as mapped on the elastic half-space. A uniform right-lateral slip of 35 mm/yr is imposed at depths greater than 10 km on this cut. Uniform strike slip and dip slip are also imposed at depths greater than 10 km on the cut representing the Laguna Salada fault, but in this case the rates of both strike and dip slip are chosen to fit the values dL/dt in Table 2. The best fit values are found to be 4.2 ± 1.4 mm/yr right-lateral slip and 7.2 ± 3.7 mm/yr normal slip. However, the rms residual for that fit (i.e., the rms difference between predicted and observed values of dL/dt) is about twice that expected from the standard deviations in Table 2. Curiously, an acceptable fit to the data is found if the dip of the Laguna Salada fault is taken to be 60° N50°E (opposite dip azimuth from the preceding model). The best fit values for slip at depth on this fault model are 4.5 ± 1.1 mm/yr right-lateral and 6.5 ± 0.8 mm/yr normal slip. The rms residual for this fit is about what one would expect given the standard deviations in Table 2. Clearly, the second model (Laguna Salada fault dipping to the northeast) is the better fit to the data. However, the Laguna Salada fault is a frontal fault on the southwest side of the Cucapah Mountains, and it is not reasonable to have a normal frontal fault dipping back under the mountains. Indeed, the sense of slip (northeast side down) indicated for the northeast dipping fault model is inconsistent with the recent southwestward facing scarps observed along the fault [*Mueller and Rockwell*, 1991]. Thus, the second model (Laguna Salada fault dipping to the northeast) is not realistic, whereas the first model (Laguna Salada fault dipping to the southwest) does not furnish an acceptable fit to the observed values of dL/dt.

The conventional model of strain accumulation for a normal fault does not furnish a satisfactory fit to the observed deformation because it predicts a zone of fault-normal contraction at the surface of the hanging-wall block above the slipping segment of the fault, whereas fault-normal extension was observed there. This is shown as follows: Suppose the fault is very long in the direction of strike. Then the two-dimensional fault model given by *Freund and Barnett* [1976, p. 670] can be employed. For the case in which normal slip at the rate b occurs uniformly on the fault plane below depth d (Figure 4) the fault-normal extension rate at the half-space surface is

$$\dot{\varepsilon}'_{11} = (2b/\pi d)(x'/d)[\sin\ \delta + (x'/d)\ \cos\ \delta]/[1 + (x/d)^2]^2 \qquad (2)$$

where δ is the fault dip and x' is the horizontal coordinate measured normal to the fault strike (Figure 4). Notice that the origin x' is directly above the top of the slipping segment and x' is reckoned positive in the direction toward the footwall block (i.e., the fault trace is at $x' = d$ ctn δ). The problem with attributing fault-normal extension across the Laguna Salada network to normal slip at depth on the Laguna Salada fault is obvious in Figure 4: Any high-angle ($\delta > 45°$) normal fault

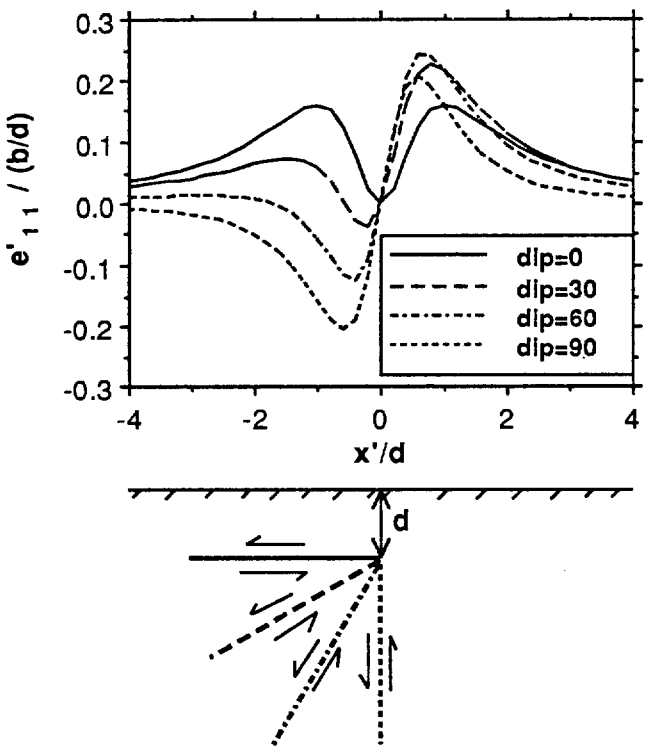

Figure 4. Fault-normal extension predicted by the conventional model of strain accumulation along a normal fault plotted as a function of horizontal distance from the top of the slipping segment of the fault. The model results are shown for four different fault dips. Uniform slip of amount b is postulated to occur at all depths greater than d in each fault model. The fault models are shown in the lower sketch.

produces a zone of fault-normal contraction, not extension, at the surface over the slipping segment of the fault. If the Laguna Salada fault were listric so that the deep slipping portion were in fact a low-angle normal fault, extension over the slipping segment could be generated. This problem was discussed in more detail by *Savage et al.* [1992, pp. 2078–2080] in connection with an analysis of strain accumulation along the Wasatch fault, Utah.

Of course, slip at depth on the Laguna Salada fault may not be the source of the observed strain accumulation. The success in modeling the strain accumulation with a northeast dip on the Laguna Salada fault suggests the possibility that the accumulation is due to slip at depth on the Cucapah fault on the northeast side of the Cucapah Mountains (Figure 1). However, the east dipping frontal fault on the east edge of the Sierra Juarez (Figure 1) is not a suitable source for the same reason that the southwest dipping Laguna Salada fault was not: fault normal contraction is induced at the surface above the hanging wall (Figure 4). Although we would prefer to attribute strain accumulation to a slip at depth on a throughgoing fault (e.g., Laguna Salada), the fact is that the geodetic measurements are not adequate to define the source of the deformation.

Discussion

The strain accumulation observed in the Laguna Salada network is essentially a 0.10 μstrain/yr N80°E uniaxial extension. That strain rate is consistent with the observed mode (roughly equal parts right-lateral and normal slip) of strain relief on the Laguna Salada fault. However, it is in contrast to the strain rates observed in the United States along the Mexican border directly north of the Laguna Salada network, essentially a 0.12 μstrain/yr north-south uniaxial contraction [*Johnson*, 1993, p. 41]. The latter estimate is derived from U.S. Geological Survey Geodolite surveys that include the triangle Carr-Jacum-229 (Figure 1). (The strain rates for that triangle alone as found from the corrected line-length data in Figure 3 are $\dot{\varepsilon}_{11} = 0.076 \pm 0.019$, $\dot{\varepsilon}_{12} = 0.046 \pm 0.012$, and $\dot{\varepsilon}_{22} = -0.031 \pm 0.020$ μstrain/yr, not significantly different from the strain rates given for the entire network in Table 3.) The nearly uniaxial north-south contraction immediately north of the Laguna Salada network reported by *Johnson* [1993] differs from the east-west extension in the Laguna Salada network by an isotropic 0.10 μstrain/yr contraction; the shear strain rates north and south of the border are comparable. Given the evidence for a normal component of slip on the Laguna Salada fault, the dominance of east-west extension south of the border is not unexpected. The dominance of north-south contraction immediately north of the border is not as easily explained.

The effect of the uniform strain observed in the Laguna Salada network is most easily visualized in terms of oblique rifting [*Withjack and Jamison*, 1986]. In a coordinate system with the 2 axis parallel to the trend of the Gulf of California-Salton trough axis (N35°W) and the 1 axis perpendicular (N55°E) to that trend, the network strain rates from Table 2 become $\dot{\varepsilon}''_{11} = 0.08 \pm 0.01$, $\dot{\varepsilon}''_{12} = -0.05 \pm 0.01$, and $\dot{\varepsilon}''_{22} = 0.00 \pm 0.01$ μstrain/yr. That is 0.08 μstrain/yr extension perpendicular to the Gulf of California-Salton trough axis, 0.10 μstrain/yr right-lateral engineering (twice the tensor) shear across the axis, and no extension along the axis. Thus, the net velocity across the rift (breadth of rift times the appropriate strain rate) will be made up of approximately equal parts extension perpendicular to the trend of the rift and shear displacement parallel to it. This interpretation applies only to the portion of the rift where the strain rates reported in Table 3 obtain.

The strain rates in Table 3 include a substantial correction intended to remove the coseismic strain increments imposed by the Imperial Valley, Victoria, Superstition Hills, and Elmore Ranch earthquakes. We show here that the coseismic correction amounts to about 30% of the accumulated strain. The strain rate equivalent of the coseismic changes is shown in Table 4. There the net coseismic strain change over the 13-year (1978–1991) interval associated solely with the calculated coseismic line-length changes in Table 2 has been divided by 13 to give an equivalent strain rate. Notice that this coseismic strain rate is almost wholly a shear. Also

Table 4. Observed, Coseismic, and Corrected Strain Accumulation Rates With Standard Deviations

	$\dot{\epsilon}_{11}$ μstrain/yr	$\dot{\epsilon}_{12}$ μstrain/yr	$\dot{\epsilon}_{22}$ μstrain/yr
Observed	0.066±0.012	0.024±0.004	0.014±0.012
Coseismic	−0.030	0.006	0.036
Corrected	0.098±0.12	0.020±0.004	−0.018±0.012

Strain rates referred to geographic coordinate system (1 axis directed east and 2 axis north).

shown in Table 4 (first row) is the strain rate that best accounts for the actually observed line length changes. Finally, the corrected strain rate in Table 4 is the previously calculated strain rate (Table 3). The observed strain rate less the equivalent coseismic strain rate is approximately equal to the corrected strain rate. That is, coseismic rupture along faults to the east of the Laguna Salada network relaxed some of the strain that had accumulated in the network over the 13-year interval, and the correction restores that strain.

The Gulf of California and its northward continuation, the Salton trough, are thought not to be the product of extension normal to the trend of the rift, but rather an alignment of adjacent pull-apart basins, each associated with an en echelon offset in the strike-slip faults (San Andreas, San Jacinto, Imperial, Cerro Prieto, and faults within the Gulf) forming the North America-Pacific plate boundary [*Larson et al.*, 1968]. That is, the Gulf of California and Salton trough are not the product of a northeast-southwest extension but rather are thought to be the consequence of nearly equal parts north-south contraction and east-west extension (i.e., right-lateral shear across the N45°W trend of the transform faults in the Gulf and Salton trough). Thus, the observation of essentially east-west uniaxial extension in the Laguna Salada network within the Salton trough is surprising. Geodetic strains observed both north of the international border in the Salton trough [*Savage et al.*, 1986] and farther south in Mexico across the Gulf of California [*Ortlieb et al.*, 1989] are consistent with simple shear (i.e., equal parts north-south contraction and east-west extension) across the vertical plane striking N45°W, the approximate trend of the transform faults in the Gulf of California and Salton trough.

Conclusions

Strain accumulation across the Laguna Salada network is roughly approximated by a uniform 0.10 μstrain/yr uniaxial east-west extension rather than the expected right-lateral shear (equal parts north-south contraction and east-west extension) across the transform faults in the Salton trough and Gulf of California. The observed strain accumulation is consistent with clear evidence for Holocene oblique (right-lateral and normal) slip on the Laguna Salada fault. An explanation for the absence of the expected north-south contraction is not apparent. We have been able to model the observed strain accumulation in the Laguna Salada network successfully by attributing it to aseismic slip at depth on the faults involved only if the Laguna Salada fault is listric.

Acknowledgments. The authors would like to thank Javier Gonzalez, Centro de Investigacion Cientifica y de Educacion Superior de Ensenada (CICESE), Ensenada, Baja California, Mexico, and Mauricio F. de la Fuente, Instituto de Geologia, Universidad Nacional de Mexico (UNAM), Mexico, for their assistance in making possible the 1991 survey of the Laguna Salada network. We are also indebted to Joann Stock and Mark Murray for critical reviews of an earlier draft of this manuscript.

References

Archuleta, R. J., A faulting model for the 1979 Imperial Valley earthquake, *J. Geophys. Res.*, *89*, 4559–4585, 1984.

Ellsworth, W. L., Earthquake history, 1769–1989, in The San Andreas Fault System, *U.S. Geol. Surv. Prof. Pap. 1515*, 153–187, 1990.

Freund, L. B., and D. M. Barnett, A two-dimensional analysis of surface deformation due to dip-slip faulting, *Bull. Seismol. Soc. Am.*, *66*, 667–675, 1976.

Humphreys, E. D., and R. J. Weldon, Kinematic constraints on the rifting of Baja California, The Gulf and Peninsula Province of the Californias, edited by J. P. Dauphin and B. R. T. Simoneit, *Mem. Am. Assoc. Pet. Geol.*, *47*, 217–229 1991.

Johnson, H. O., Techniques and studies in crustal deformation, Ph.D. thesis, 213 pp., Univ. of Calif., San Diego, 1993.

Larsen, S., R. Reilinger, H. Neugebauer, and W. S. Strange, Global Positioning System measurement of deformations associated with the 1987 Superstition Hills earthquake: Evidence for conjugate faulting, *J. Geophys. Res.*, *97*, 4885–4902, 1992.

Larson, R. L., H. W. Menard, and S. Smith, Gulf of California: A result of ocean floor spreading and transform faulting, *Science*, *161*, 781–784, 1968.

Lisowski, M., and W. H. Prescott, Deformation near the epicenter of the 9 June 1980 M_L = 6.2 Victoria, Mexico, earthquake, in *Fourth Symposium on the Cerro Prieta Geothermal Field, Baja California, Mexico*, Lawrence Berkeley Laboratory, Berkeley, Calif., 1984.

Mueller, K. J., and T. K. Rockwell, Late Quaternary structural evolution of the western margin of the Sierra Cucapa, northern Baja California, in The Gulf and Peninsula Province of the Californias, edited by J. P. Daughin and B. R. T. Simoneit, *Mem. Am. Assoc. Pet. Geol.*, *47*, 249–260, 1991.

Ortlieb, L., J. C. Ruegg, J. Angelier, B. Colletta, M. Kasser, and P. Lesage, Geodetic and tectonic analysis along an active plate boundary: The central Gulf of California, *Tectonics*, *8*, 429–441, 1989.

Savage, J. C., Strain accumulation in western United States, *Annu. Rev. Earth Planet. Sci.*, *11*, 11–43, 1983.

Savage, J. C., and W. H. Prescott, Precision of Geodolite distance measurements for determining fault movements, *J. Geophys. Res.*, *78*, 6001–6008, 1973.

Savage, J. C., W. H. Prescott, and G. Gu, Strain accumulation in southern California, 1973–1984, *J. Geophys. Res.*, *91*, 7455–7473, 1986.

Savage, J. C., M. Lisowski, and W. H. Prescott, Strain accumulation across the Wasatch fault near Ogden, Utah, *J. Geophys. Res.*, *97*, 2071–2083, 1992.

Silver, P., and T. Masuda, A source extent analysis of the Imperial Valley earthquake of October 15, 1979, and the Victoria earthquake of June 9, 1980, *J. Geophys. Res.*, *90*, 7639–7651, 1985.

Withjack, M. O., and W. R. Jamison, Deformation produced by oblique rifting, *Tectonophysics*, *126*, 99–124, 1986.

W. K. Gross, N. E. King, M. Lisowski, and J. C. Savage, U.S. Geological Survey, 345 Middlefield Road, MS/977, Menlo Park, California 94025.

(Received January 20, 1994; revised May 16, 1994; accepted June 8, 1994.)